FINITE ELEMENT ANALYSIS OF SLABS-ON-GRADE USING A VARIETY OF SUPPORT MODELS

A. M. Ioannides, Research Assistant, University of Illinois
M. R. Thompson, Professor of Civil Engineering, University of Illinois
E. J. Barenberg, Professor of Civil Engineering, University of Illinois

The Finite Element Method has been a very powerful tool for the analysis of slab-on-grade type pavements in the last two decades. A number of programs have been developed which treat the slab as an elastic plate and characterize foundation support either as a dense liquid or as an elastic solid. This paper describes the development of an expanded and revised version of ILLI-SLAB, which now incorporates four subgrade idealizations: the Winkler dense liquid, the Boussinesq elastic solid, the stress dependent resilient subgrade and the Vlasov two-parameter foundation. Comparative studies are greatly facilitated and results from numerous runs are presented to illustrate the scope of the program's applicability. The efficient utilization of ILLI-SLAB is ensured by adherence to guidelines established during several convergence studies described.

Introduction

Slab-on-grade pavements belong to that broad category at the interface of structural and geotechnical engineering, commonly referred to as soil-structure interaction problems. For the analysis of such problems, the Finite Element Method (F.E.M.) has been a favorite among engineers in the last two decades. Its major attribute is flexibility in modeling a variety of pavement systems, loaded by any combination of loads, applied anywhere on the slab surface. As in numerous other engineering applications, the pavement slab is treated as an elastic plate, but it is the response of the supporting soil medium that is the governing consideration. The inherent complexity of real soils has led to the development of a number of idealized models, which attempt to provide a useful description of certain aspects of soil response under a specific set of loading and boundary conditions.

This paper describes the development of a finite element program which may be used for slab-on-grade analysis using a variety of support models. This is an expanded and revised version of ILLI-SLAB, developed and extensively used at the University of Illinois. The new version incorporates three models in addition to the original dense liquid (Winkler) foundation. These are the stress dependent resilient subgrade, the Boussinesq elastic half-space, and the Vlasov two-parameter idealization. Results from several runs are presented to illustrate the scope of the program's application and to establish guidelines for its efficient utilization.

ILLI-SLAB

ILLI-SLAB was developed at the University of Illinois for structural analysis of jointed, one- or two-layer concrete pavements with load transfer systems (1). The original ILLI-SLAB model is based on the classical theory of a medium-thick plate on a Winkler foundation and employs the 4-noded, 12-dof plate bending element known as ACM or RPB12 (2). The Winkler type subgrade is modeled as a uniform, distributed subgrade through an equivalent mass formulation (3). This is a more realistic representation than the four concentrated spring elements used in other similar programs. A work equivalent load vector is used (2). The model has been verified by comparison with available theoretical solutions and results from experimental studies (4,1,5).

Recently, ILLI-SLAB has been improved by expanding its capabilities to include modeling of other types of foundations, in addition to the original dense liquid formulation (6). Modifications to improve its accuracy and ease of application, and to enhance the beneficial interpretation of its results have been presented by the authors in an earlier paper (7).

ILLI-SLAB Stress Dependent Model

A stress dependent model developed and incorporated into ILLI-SLAB to account for subgrade behavior in response to rapidly moving, repeated loads, has been previously described (7). Only its highlights will be summarized here. This model is based on the concept of the Resilient Modulus of Subgrade Reaction, K_R (8), which is analogous to the modulus of subgrade reaction, k, from the static plate load test, but is defined by:

$$K_R = \frac{\text{applied plate pressure}}{\text{resilient (recoverable) plate deflection}} \quad (1)$$

Algorithms were developed (5) relating K_R and the level of resilient deflection using ILLI-PAVE (9), a finite element program in which subgrade material stress-strain relations from repeated, impulse-type, tests (10) are employed. These algorithms form a part of an iterative scheme in ILLI-SLAB, according to which a selected initial value of K_R (depending on subgrade type) is corrected after each iteration, to correspond to the deflection level obtained. After two or three iterations, the values of K_R before and after the last iteration are only negligibly different.

To illustrate the impact of the introduction of the resilient subgrade model, a number of demonstration runs were performed (7). The conclusions reached from these runs were as follows:

1. The proposed change to a resilient modulus of subgrade reaction characterization has only a minor effect on load transfer efficiency and deflection or stress reduction obtained when a series of interconnected slabs are used.
2. The resilient subgrade leads to lower calculated deflections and stresses, with stresses affected to a smaller extent than deflections. A more significant effect was noted for more severe loads and/or less competent pavement systems;
3. The effect of the iterative scheme is not dramatic, probably since the stress dependent algorithms employed in ILLI-SLAB were developed by simulating rigid plate tests. ILLI-SLAB can accommodate refined K_R algorithms, corresponding to a more typical pavement system relative stiffness range, when these are developed.

The Elastic Solid Option in ILLI-SLAB

The elastic solid idealization has been added to ILLI-SLAB so that both the elastic solid and dense liquid models would be available in a single finite element program. Direct comparisons can now be made between the two models with respect to execution costs, computer storage requirements, accuracy, and factors affecting the efficiency of the finite element mesh, as well as comparisons between pavement system responses in each case. The elastic solid option in ILLI-SLAB is based upon a procedure described by Cheung and Zienkiewicz (11). They assumed a piecewise uniform approximation to the subgrade reaction, and formed the subgrade stiffness matrix by inverting the flexibility matrix obtained using Boussinesq's theory. This concept had also been used by Pickett, et al. (12) in a finite difference solution of the same problem.

Since it is desirable that meshes consisting of elements of unequal size should be admitted, an equation for the deflection under the corner of a uniformly loaded rectangular area over an elastic solid foundation, given by Giroud (13) was used in the ILLI-SLAB formulation. The following expression was derived for deflection w_{ii}, at node i due to a uniform pressure q_i over the rectangular area of influence surrounding this node:

$$w_{ii} = \frac{1-\mu_s^2}{E_s \pi} \left\{ \frac{1}{\sum_{j=1}^{m} (SIDEL_j * SIDES_j)} * \sum_{j=1}^{m} SIDES_j \, f_j(\alpha) \right\} Q_i \quad (2)$$

where:

m: number of contributary quadrants surrounding node i (1, 2 or 4);
$SIDEL_j$: long side of contributary quadrant j;
$SIDES_j$: short side of contributary quadrant j;
α: $SIDEL_j$ / $SIDES_j \geq 1.0$;

$$f_j(\alpha) = \{\ln(\alpha + \sqrt{1+\alpha^2}) + \alpha \ln(\frac{1+\sqrt{1+\alpha^2}}{\alpha})\}$$

Q_i: total resultant reaction force at node i,
E_s: subgrade Young's modulus;
μ_s: subgrade Poisson's ratio.

Similarly, vertical displacement w_{ni}, at a node n due to the uniformly loaded rectangular area surrounding node i, may be written as:

$$w_{ni} = \frac{1-\mu_s^2}{E_s \pi} \{\frac{1}{r_{ni}}\} Q_i \quad (3)$$

where r_{ni} is the distance between n and i. Note that while Eqn. 2 is exact, Eqn. 3 is only an approximation, since the uniformly loaded rectangular area is replaced by the resultant total load Q_i, rather than performing an exact integration.

Cheung and Zienkiewicz (11) claim that this is an adequate approximation (error less than about 5%) but this is only true for square areas of influence ($\alpha = 1.0$). Significant deterioration of the approximation occurs for other values of the aspect ratio (Fig. 1).

Convergence Studies With ILLI-SLAB Elastic Solid

To validate the elastic solid finite element model in ILLI-SLAB, examine the limits of its applicability and establish guidelines for potential users, several runs were performed. Results are compared to available closed-form solutions (14) and are discussed below.

Slab Size Effect. The non-dimensional ratio (L/ℓ_e), of slab length to the radius of relative stiffness, is used to characterize this effect, using square slabs divided into square elements, and loaded by one small square interior load. The radius of relative stiffness for a plate on an elatic solid foundation is defined by:

$$\ell_e = \sqrt[3]{\frac{Eh^3 (1-\mu_s^2)}{6 E_s (1-\mu^2)}} \quad (4)$$

The slab used here has a rather low ℓ_e value (63.5 cm; 25 in.) for practical reasons. The range of (L/ℓ_e) examined is 1.4 to 6.9.

Figure 1. Evaluation of the approximation proposed by Cheung and Zienkiewicz.

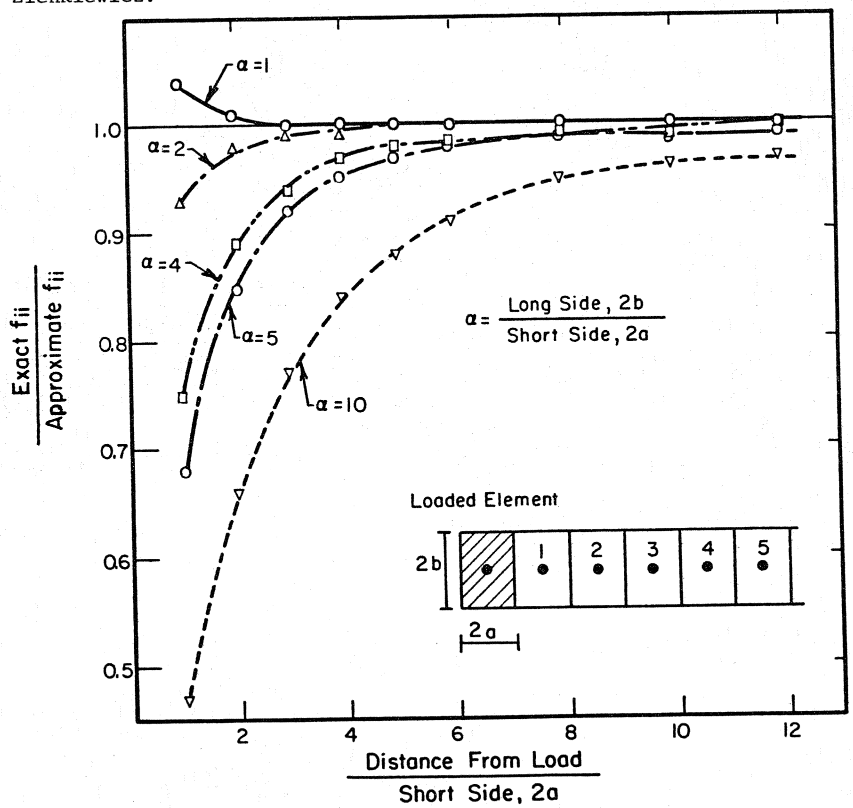

Figure 2. Effect of slab size (ILLI-SLAB elastic solid).

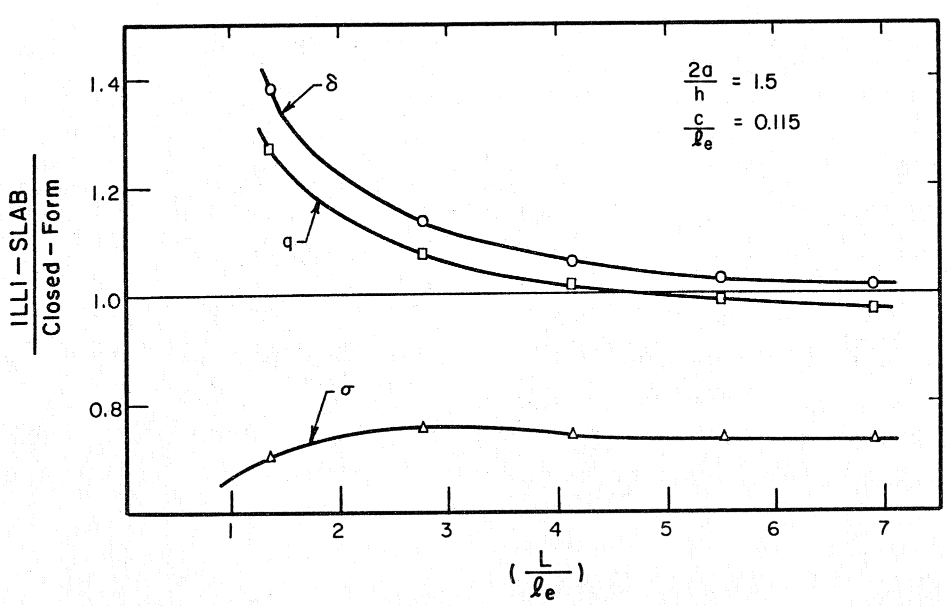

A non-dimensional plot of ILLI-SLAB results is shown in Fig. 2. As expected, deflection and subgrade stress converge to the infinite slab response from above, exhibiting a typical "punch-like" behavior at small slab sizes. On the other hand, bending stress converges from below, and is much less sensitive to such changes. As shown below, discrepancies observed between the large (L/ℓ_e) and infinite slab responses can be attributed to mesh fineness effects. These discrepancies aside, bending stress converges to the large slab value at (L/ℓ_e) of about 3.0. For deflection and subgrade stress, a much higher value (about 7.0) is required. These values are comparable with those obtained for the dense liquid finite element solution (5).

Mesh Fineness Effect. This effect is characterized by the non-dimensional ratio (2a/h), where 2a is the length of the (square) elements and h is the slab thickness. For one of the cases solved above $(L/\ell_e = 4.2)$, responses were calculated using finer and coarser meshes.

The non-dimensional graphical representation of the results (Fig. 3) shows that all three responses converge from below. Bending stress is much more sensitive to mesh fineness than deflection and subgrade stress. A finer mesh would eliminate the discrepancies observed in Fig. 2. Similarly, the discrepancies shown in Fig. 3 can be explained in terms of the slab size effect. The required values of (2a/h) for good results are as follows:

Deflection :	(2a/h) = 1.5
Subgrade Stress:	(2a/h) = 0.9
Bending Stress :	(2a/h) = 0.8.

Effect of Size of Loaded Area. The non-dimensional ratio (c/ℓ_e) of the length of the (square) load divided by the radius of relative stiffness was used to quantify this effect. Several runs were performed for another of the cases considered above. Total applied load, P, was held constant, but was distributed on an increasingly larger square area.

The results are plotted in Fig. 4. It is observed that all three responses increase in comparison to their closed-form counterparts, with bending stress being much more sensitive to this effect. Similar behavior was observed for the dense liquid model in ILLI-SLAB (5). This is associated with a mesh fineness effect in the loaded region, in view of the way the F.E.M. converts applied distributed loads, to concentrated, nodal force components. Another contributing factor is the fact that closed-form solutions are only the first one or two terms of an infinite series. Note that the absolute values of the three responses decrease as (c/ℓ_e) increases.

Effect of Element Aspect Ratio. Element aspect ratio, α, defined as the ratio of the long side of the element to its short side, is particularly important in the elastic solid model, due to the approximation mentioned above. In a series of runs performed to investigate this effect, the slab was divided into a number of identical elements of a given aspect ratio. This may have a more pronounced effect than a typical mesh which uses only a few high aspect ratio elements.

Figure 5 presents results from these runs in a non-dimensional plot. The deterioration in accuracy of subgrade stress and bending stress is very significant. This effect persists far beyond the loaded region. If at all possible, aspect ratios greater than 2 should be avoided, especially close to the loads or in the region of expected critical response.

Investigation of the k-Surface

With the addition of the Elastic Solid option in ILLI-SLAB, the program incorporates both fundamental subgrade idealizations (viz. Winkler and Boussinesq foundations) in a usable package. This opens up new possibilities for comparative studies. The investigation presented below illustrates the broad scope of such analyses.

The concept of the k-surface will be introduced at this point. This is an imaginary surface showing the spatial distribution (x,y) of the subgrade modulus, k, under a slab resting on an elastic solid foundation. Using a constant k at all points under the slab, as is the conventional practice, yields a k-surface that forms a horizontal plane. It might be reasonably expected that with appropriate modifications of this surface, the dense liquid and elastic solid may be better correlated.

The value of k(x,y) may be obtained, by definition, from:

$$k(x,y) = q(x,y) \;/\; w(x,y) \tag{5}$$

where q(x,y) and w(x,y) are the values of subgrade stress and deflection calculated for any given location, using the plate on elastic solid theory. Thus, it is possible to perform an elastic solid run on ILLI-SLAB and back-calculate nodal values of k by applying Eqn. 5. Since ILLI-SLAB allows node-by-node specification of subgrade modulus values, the Winkler option may then be employed to reproduce the Boussinesq results.

One of the cases in the mesh fineness study was selected for this investigation. For this case (2a/h) is 0.9 and (L/ℓ_e) is 4.151, i.e. mesh fineness and slab size effects are minimized. The remaining parameters are shown in Table 1. The process outlined above was applied to each of the three fundamental cases of loading: interior, edge, and corner. The results of the Elastic Solid option were reproduced fairly accurately by the Winkler option for these cases. Table 1 presents comparisons of the maximum responses obtained. It is interesting to note that for all three loading conditions dense liquid foundation stresses and deflections are higher than for the elastic solid subgrade. Furthermore, the interior condition is the easiest to reproduce, while corner loading gives the most unsatisfactory comparison, especially with respect to bending stresses. This clearly illustrates the primary deficiency of the discontinuous Winkler model, namely its assumption that soil elements beyond the slab edges do not provide any support. Figures 6 through 8 show contours of the k-surface in each of the three cases investigated. Edge and corner effects on k-values are extremely pronounced.

Carlton and Behrmann (15) suggested using a flat k-surface, with the value of k determined from the deflection basin obtained under a slab on an elastic solid. Using results from laboratory model tests, they calculated an "equivalent k value" from the relationship:

$$k = P/V \tag{6}$$

where:

P : total applied load;
V : volume of deflection basin.

Figure 3. Effect of mesh fineness (ILLI-SLAB elastic solid).

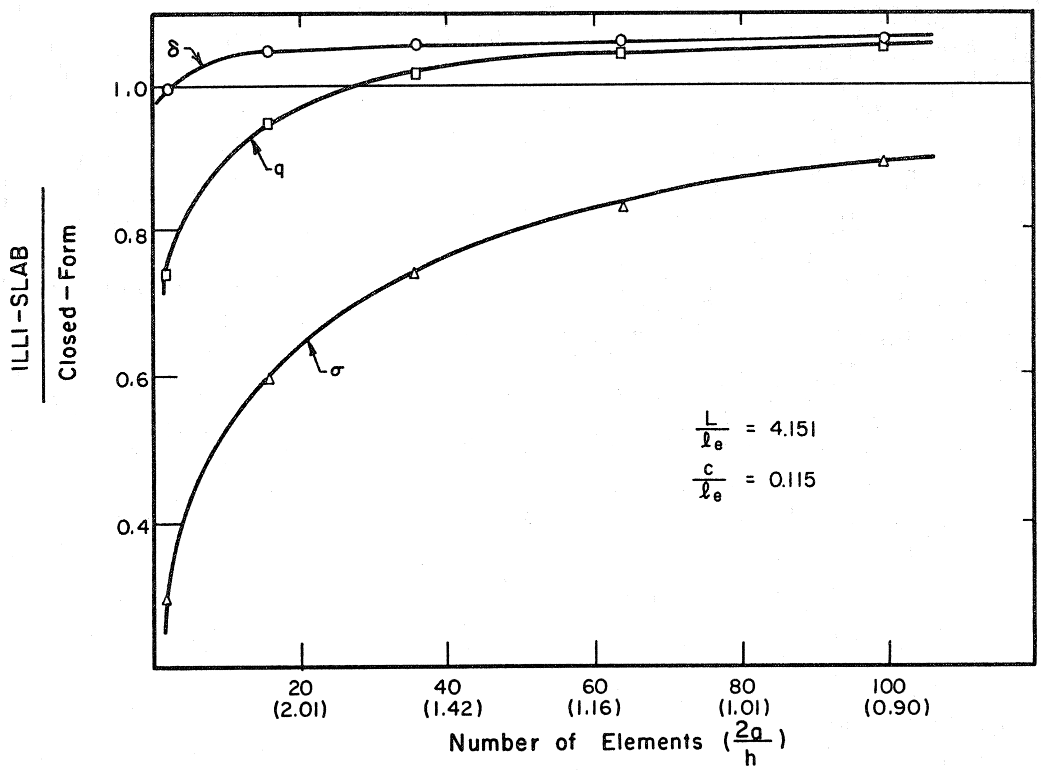

Figure 4. Effect of size of loaded area (ILLI-SLAB elastic solid).

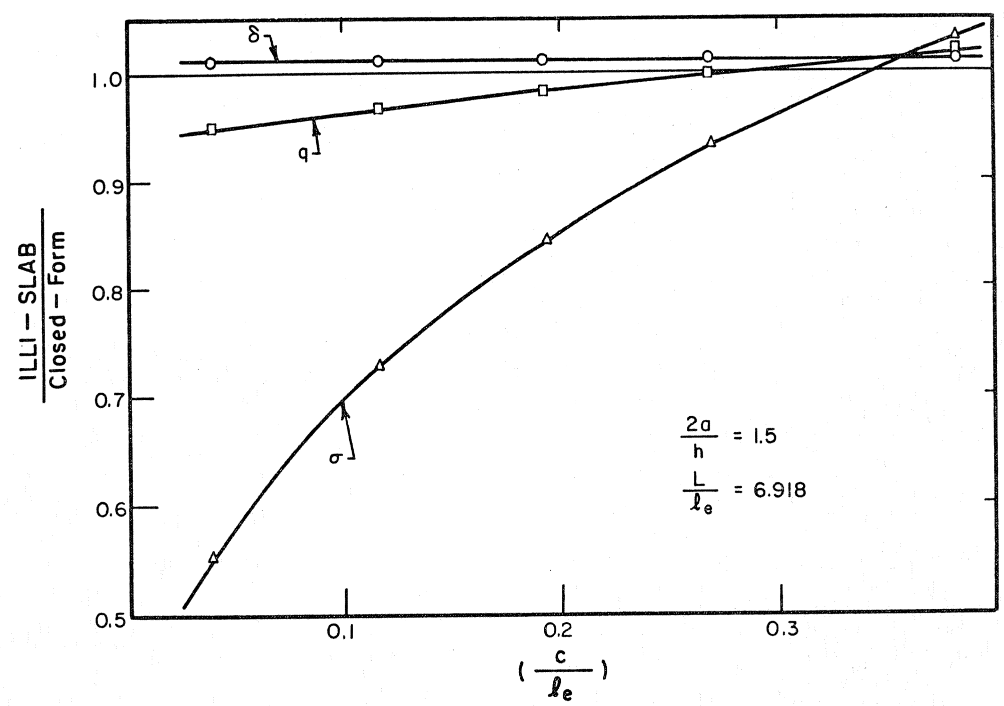

Table 1. Maximum responses for dense liquid and elastic solid.

LOAD PLACEMENT	Deflection (mm)			Subgrade Stress (kPa)			Bending Stress (kPa)		
	E.S.	D.L.	D.L./E.S.	E.S.	D.L.	D.L./E.S.	E.S.	D.L.	D.L./E.S.
Interior	0.0070	0.0071	1.01	1.80	1.81	1.01	70.69	71.10	1.01
Edge	0.0121	0.0135	1.11	12.39	13.77	1.11	136.15	140.00	1.03
Corner	0.0199	0.0242	1.22	60.80	73.49	1.22	56.15	83.16	1.48

Notes:

Slab: 274x274 cm ($L/\ell_e = 4.151$)

Mesh: 10x10 @ 27.4 cm. ($2a/h = 0.9$)

$h = 30$ cm

$E = 20.7$ GPa $\mu = 0.15$

$E_s = 27.56$ MPa $\mu_s = 0.45$

$\ell_e = 66.1$ cm

$k = q/w$ (back-calculated) D.L.: Dense Liquid

A = 7.5x7.5 cm @689 kPa E.S.: Elastic Solid

Table 2. k comparisons.

(a) EQUIVALENT k VALUES: ELASTIC SOLID RUNS

LOAD PLACEMENT	EQUIVALENT k (kPa/cm)	k/k_{corner}	k/k_{edge}
Interior	1257	0.66	0.83
Edge	1520	0.79	1.00
Corner	1916	1.00	1.26

(b) DENSE LIQUID RESPONSES USING EQUIVALENT k VALUES

LOAD PLACEMENT	ASSUMED k (kPa/cm)	BACK-CALCULATED k (kPa/cm)		DEFLECTION		SUBGRADE STRESS		BENDING STRESS	
		w/o −ve δ	w/ −ve δ	(mm)	D.L./E.S.	(kPa)	D.L./E.S.	(kPa)	E.L./E.S.
Interior	1257	1266	1266	0.0076	1.08	0.97	0.54	75.9	1.07
Edge	1520	1226	1515	0.0228	1.88	3.52	0.28	154.7	1.14
Corner	1916	1363	1881	0.0465	2.34	9.06	0.15	101.7	1.81

Notes: Mesh: 10x10 @ 27.4 cm $E_s = 275.6$ MPa

L = 274x274 cm $\mu_s = 0.45$

h = 30 cm E.S.: Elastic Solid (see Table 1)

E = 20.7 GPa; $\mu = 0.15$ D.L.: Dense Liquid

A = 7.5x7.5 cm @ 689 kPa Equivalent k from (Eqn. 5)

Figure 5. Deterioration of accuracy with aspect ratio (ILLI-SLAB elastic solid).

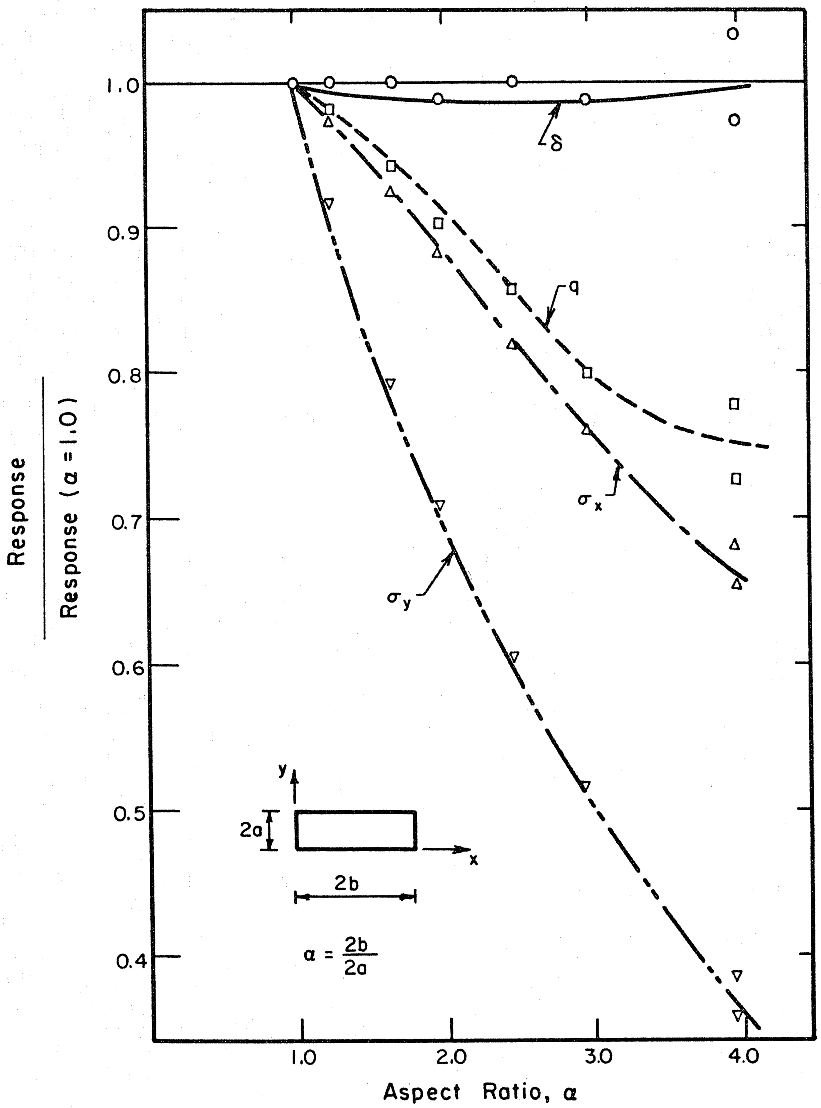

A calculation as indicated by Eqn. 6 may easily be performed using ILLI-SLAB elastic solid results. The volume of the deflection basin is simply the sum of nodal deflections times the area of influence surrounding each node. For the three cases analyzed above, this approach yielded the equivalent k values shown in Table 2(a). An increase in k is observed as the load moves from the interior to the edge and then to the corner of the slab. Carlton and Behrmann (15) noted that the equivalent k value for interior loading was found to be "approximately half the value of k measured at the edge and at the corner," the latter two being practically the same. ILLI-SLAB results suggest a more gradual increase in k.

Using the equivalent k values back-calculated from Eqn. 6 in dense liquid analyses, leads to the maximum responses given in Table 2(b). Agreement between dense liquid and elastic solid results obtained using a flat k-surface is much less satisfactory than when variable nodal k values are employed (Table 1). Note, however, that when negative deflections are included in the determination of the deflection basin volume, the equivalent k value from a dense liquid analysis is nearly identical to the value assumed for that run. Equation 6 is merely a condition of equilibrium between the applied load and the subgrade reactions and is a valid method of estimating an equivalent k under the slab. This finding is significant with respect to non-destructive pavement evaluation methods which generate a deflection profile (e.g. Falling Weight Deflectometer, Road Rater, etc.).

ILLI-SLAB Two-Parameter Model

To examine the applicability of Vlasov's two-parameter model (16) in the analysis of slabs-on-grade, a finite element formulation was used to derive the subgrade stifness matrices for this model. The formulation, which has now been incorporated into ILLI-SLAB, is outlined below.

In deriving the stiffness matrix for a Winkler type subgrade, Tabatabaie, et al. (4) used the principle of virtual work. In the present formulation, the concept of strain energy was used instead, to provide a check on the Winkler subgrade stiffness matrix derived in Ref. (4), and obtain the additional stiffness matrices required to define a Vlasov type idealization. For such a

Figure 6. Contours of k-surface (interior loading).

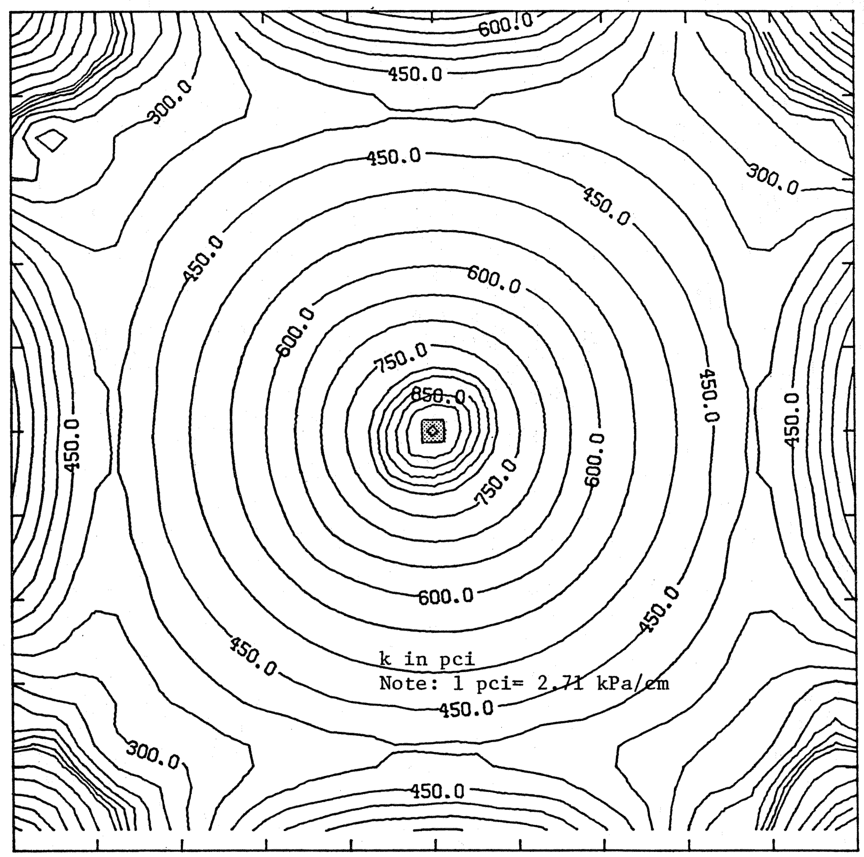

Figure 7. Contours of k-surface (edge loading).

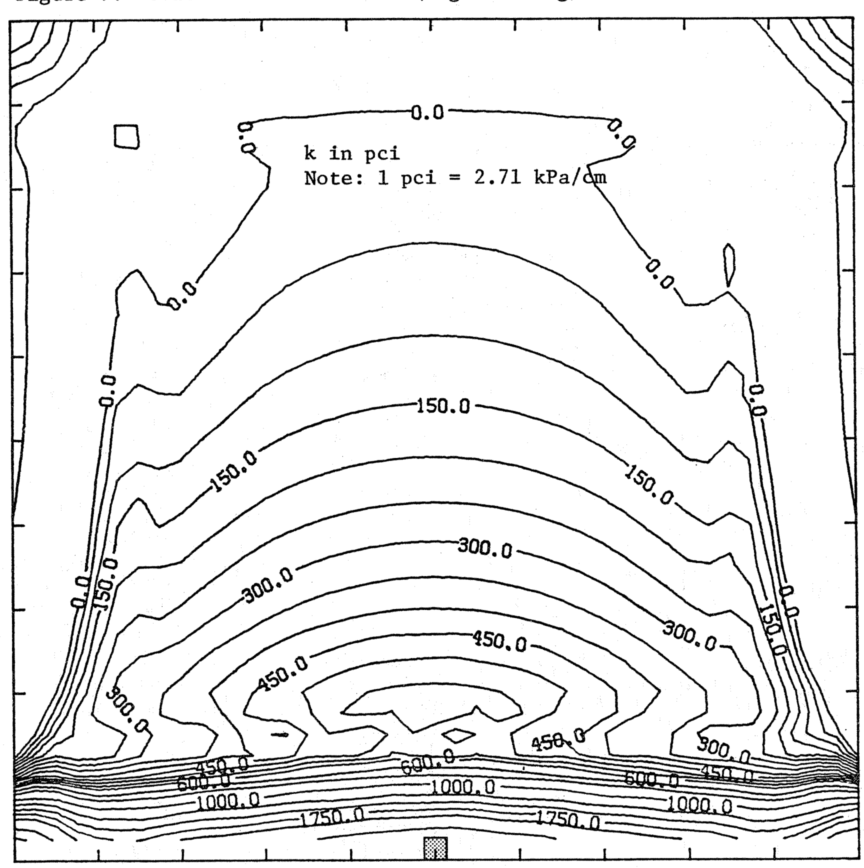

Figure 8. Contours of k-surface (corner loading).

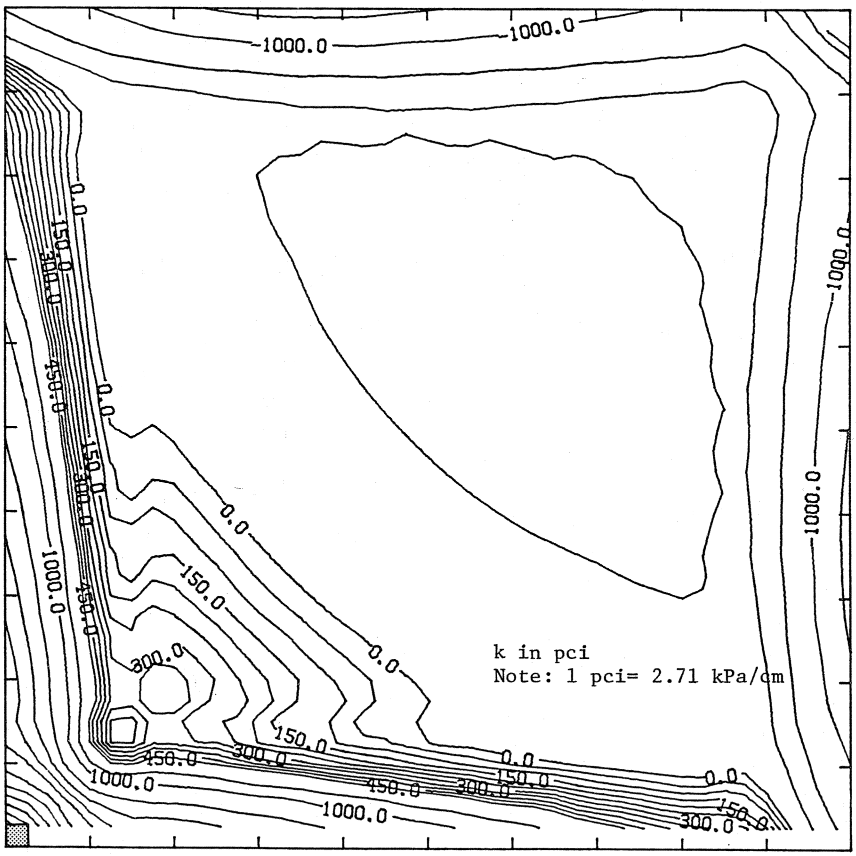

foundation, subgrade reaction, q, is related to surface deflection, w, through:

$$q = kw - G\frac{\partial^2 w}{\partial x^2} - G\frac{\partial^2 w}{\partial y^2} \tag{7}$$

where:

G : foundation constant describing the shear interaction between adjacent springs (assumed to be equal in x- and y-directions).

Note that if G is set to zero, the Vlasov foundation reduces to the Winkler dense liquid. The total strain energy for an element 2aX2b in size located at the interior of a finite element mesh may be written as:

$$U = \int_0^{2a}\int_0^{2b} \{\frac{1}{2} kw^2 + \frac{1}{2} G(\frac{\partial w}{\partial x})^2 + \frac{1}{2} G(\frac{\partial w}{\partial y})^2\} dx\, dy \tag{8}$$

Stiffness matrices corresponding to each of the three terms in Eqn. 8 are obtained using Castigliano's theorem and the assumed displacement function.

In accordance with the derivation for the original version of ILLI-SLAB, which employs the 4-noded 12-dof plate bending element (known as ACM or RPB12), the nodal displacements, {d}, consisting of w, θ_x (=$-\partial w/\partial x$) and θ_y (= $\partial w/\partial y$) may be related to the vertical deflection at any point through:

$$w_{1X1} = [N]_{1X12}\{d\}_{12X1} \tag{9}$$

where [N] is the row vector of shape functions for this element.

Applying Castigliano's theorem to each of the three contributions to the total strain energy, the following expressions for typical stiffness matrix terms are derived, using the shape functions in Eqn. 9, for an element of size 2ax2b located away from the plate edges:

Winkler Term

$$K_{i,j}=k\int_0^{2a}\int_0^{2b} N_i \cdot N_j\, dx\, dy \quad (i=1,12;\ j=1,12) \tag{10}$$

Shear Interaction x-Term

$$K_{i,j}=G\int_0^{2a}\int_0^{2b} \frac{\partial N_i}{\partial x} \cdot \frac{\partial N_j}{\partial x}\, dx\, dy \quad (i=1,12;\ j=1,12) \tag{11}$$

Shear Interaction y-Term

$$K_{i,j}=G\int_0^{2a}\int_0^{2b} \frac{\partial N_i}{\partial y} \cdot \frac{\partial N_j}{\partial y}\, dx\, dy \quad (i=1,12;\ j=1,12) \tag{12}$$

These stiffness matrices were evaluated using computerized numerical integration, and are presented in Table 3. The stiffness matrix for the Winkler term is identical to that derived by Tabatabaie, et al. (4). The stiffness matrices for the two shear interaction terms are more accurate than those presented by Severn (17), which contained several numerical and typographical errors.

Note that in addition to the distributed reaction q Eqn. 7, concentrated reactions arise at the plate boundaries (18). These reflect the interaction between subgrade elements under the slab, and those beyond the slab boundaries. Yang

Table 3. Stiffness matrices for two-parameter foundation.

(a) <u>Winkler Term</u>

$$
\frac{kab}{44{,}100}
\begin{bmatrix}
24178 & & & & & & & & & & & \\
-6454\,b & 2240\,b^2 & & & & & & & & & & \\
6454\,a & -1764\,ab & 2240\,a^2 & & & & & & & & & \\
8582 & -3836\,b & 2786\,a & 24178 & & & & & & & & \\
3836\,b & -1680\,b^2 & 1176\,ab & 6454\,b & 2240\,b^2 & & & & & \text{SYMMETRIC} & & \\
2786\,a & -1176\,ab & 1120\,a^2 & 6454\,a & 1764\,ab & 2240\,a^2 & & & & & & \\
8582 & -2786\,b & 3836\,a & 2758 & 1624\,b & 1624\,a & 24178 & & & & & \\
-2786\,b & 1120\,b^2 & -1176\,ab & -1624\,b & -840\,b^2 & -784\,ab & -6454\,b & 2240\,b^2 & & & & \\
-3836\,a & 1176\,ab & -1680\,a^2 & -1624\,a & -784\,ab & -840\,a^2 & -6454\,a & 1764\,ab & 2240\,a^2 & & & \\
2758 & -1624\,b & 1624\,a & 8582 & 2786\,b & 3836\,a & 8582 & -3836\,b & -2786\,a & 24178 & & \\
1624\,b & -840\,b^2 & 784\,ab & 2786\,b & 1120\,b^2 & 1176\,ab & 3836\,b & -1680\,b^2 & -1176\,ab & 6454\,b & 2240\,b^2 & \\
-1624\,a & 784\,ab & -840\,a^2 & -3836\,a & -1176\,ab & -1680\,a^2 & -2786\,a & 1176\,ab & 1120\,a^2 & -6454\,a & -1764\,ab & 2240\,a^2
\end{bmatrix}
$$

(b) <u>Shear Interaction x-Term</u>

$$
\frac{G(b/a)}{88{,}200}
\begin{bmatrix}
38640 & & & & & & & & & & & \\
-9240\,b & 3360\,b^2 & & & & & & & & & & \\
5880\,a & 0 & 15680\,a^2 & & & & & & & & & \\
14280 & -5460\,b & 2940\,a & 38640 & & & & & & & & \\
5460\,b & -2520\,b^2 & 0 & 9240\,b & 3360\,b^2 & & & & & \text{SYMMETRIC} & & \\
2940\,a & 0 & 7840\,a^2 & 5880\,a & 0 & 15680\,a^2 & & & & & & \\
-38640 & 9240\,b & -5880\,a & -14280 & -5460\,b & -2940\,a & 38640 & & & & & \\
9240\,b & -3360\,b^2 & 0 & 5460\,b & 2520\,b^2 & 0 & -9240\,b & 3360\,b^2 & & & & \\
5880\,a & 0 & -3920\,a^2 & 2940\,a & 0 & -1960\,a^2 & -5880\,a & 0 & 15680\,a^2 & & & \\
-14280 & 5460\,b & -2940\,a & -38640 & -9240\,b & -5880\,a & 14280 & -5460\,b & -2940\,a & 38640 & & \\
-5460\,b & 2520\,b^2 & 0 & -9240\,b & -3360\,b^2 & 0 & 5460\,b & -2520\,b^2 & 0 & 9240\,b & 3360\,b^2 & \\
2940\,a & 0 & -1960\,a^2 & 5880\,a & 0 & -3920\,a^2 & -2940\,a & 0 & 7840\,a^2 & -5880\,a & 0 & 15680\,a^2
\end{bmatrix}
$$

(c) <u>Shear Interaction y-Term</u>

$$
\frac{G(a/b)}{88{,}200}
\begin{bmatrix}
38640 & & & & & & & & & & & \\
-5880\,b & 15680\,b^2 & & & & & & & & & & \\
9240\,a & 0 & 3360\,a^2 & & & & & & & & & \\
-38640 & 5880\,b & -9240\,a & 38640 & & & & & & & & \\
-5880\,b & -3920\,b^2 & 0 & 5880\,b & 15680\,b^2 & & & & & \text{SYMMETRIC} & & \\
-9240\,a & 0 & -3360\,a^2 & 9240\,a & 0 & 3360\,a^2 & & & & & & \\
14280 & -2940\,b & 5460\,a & -14280 & -2940\,b & -5460\,a & 38640 & & & & & \\
-2940\,b & 7840\,b^2 & 0 & 2940\,b & -1960\,b^2 & 0 & -5880\,b & 15680\,b^2 & & & & \\
-5460\,a & 0 & -2520\,a^2 & 5460\,a & 0 & 2520\,a^2 & -9240\,a & 0 & 3360\,a^2 & & & \\
-14280 & 2940\,b & -5460\,a & 14280 & 2940\,b & 5460\,a & -38640 & 5880\,b & 9240\,a & 38640 & & \\
-2940\,b & -1960\,b^2 & 0 & 2940\,b & 7840\,b^2 & 0 & -5880\,b & -3920\,b^2 & 0 & 5880\,b & 15680\,b^2 & \\
5460\,a & 0 & 2520\,a^2 & -5460\,a & 0 & -2520\,a^2 & 9240\,a & 0 & -3360\,a^2 & -9240\,a & 0 & 3360\,a^2
\end{bmatrix}
$$

(19) proposed an iterative scheme to account for these reactions. This inevitably prolongs execution time. Other possible approaches are discussed in Ref. (6). The concentrated boundary reactions will be more pronounced for slabs of high rigidity.

Model Behavior

To investigate the major aspects of the behavior of the Vlasov finite element model in ILLI-SLAB, a number of computer runs were performed (20). A square slab with square elements was used to avoid any problems related to plate or element aspect ratios. The slab was loaded by a single, interior, square load. The concentrated boundary reactions (which in most cases considered should be fairly small) were not accounted for in these runs. This is considered to have only a minor effect on the qualitative conclusions reached below.

Mesh Fineness Effect. A series of runs were performed in which the slab was divided into a number of elements, ranging from 16 to 400. These indicated that deflections are much less sensitive to mesh fineness than bending stresses. Furthermore, convergence is from above for deflections, and from below for bending stresses. Figure 9 shows the bending stress results in a graphical form. A mesh fineness ratio (2a/h) of about 0.8 is required for accurate bending stresses.

Effect of k for Constant G. For one particular slab under interior loading, a series of runs were performed in which the value of the modulus of subgrade reaction was varied between fairly wide limits. The runs were otherwise identical to each other.

Typical results are presented in Figures 10 and 11. These confirm that as k increases, maximum plate deflection and bending stress decrease. It is also observed that as k increases, the deflection and bending stress at the plate edge both decrease. Maximum subgrade stress increases with k, while subgrade stress at the plate edge decreases. For low values of k, the deflection profile is fairly flat, indicating the predominance of G, whose effect -as indicated by Mahanyi (21)- is to transfer some of the response from the interior to the edges. On the other hand, increasing the value of k tends to concentrate the bulk of the deflection under the interior load; the edges deflect progressively less, and eventually lift up and lose contact with the soil. A similar trend is observed for bending stresses, but the effects are considerably less pronounced.

Effect of G for Constant k. In the analyses in this section, the value of the shear parameter, G, is varied, while all other aspects of the runs are kept unaltered. Mahanyi [21] had noted that as G increases maximum deflection decreases, and this is confirmed by results obtained in this study. Maximum bending stress also decreases as G increases. The effect of G on the deflection profile is to flatten it out (Fig. 12), confirming both Mahanyi's observation and comments made above. The effect of increasing G on bending stresses is to increase the relative significance of stresses at the interior, although this effect is very small in magnitude.

An increase in G leads to higher subgrade stresses both at the interior and at the edges of the slab. The increase at the edge, however, is considerably smaller, leading to increased relative significance of interior stresses. This is quite unexpected, and is the opposite of the effect on the deflection profile.

In general, it may be concluded that k and G affect both the shape and the magnitude of the deflection profile. A flatter deflection profile may be obtained by decreasing k or increasing G. A reduction in maximum deflection is achieved by increasing either parameter. These effects are much more pronounced in response to changes in k. To obtain the same changes produced by doubling k, G must be increased by 2 to 3 orders of magnitude. When the two parameters are considered individually, however, a given change in k produces predominantly a magnitude effect; for a given change in G, the shape effect is slightly more important than the magnitude effect.

Comparison of Winkler, Vlasov and Elastic Solid Models

Using a trial-and-error process, the Vlasov and Elastic Solid deflection profiles can be matched. Comparisons of response profiles for the three models (Winkler, Elastic Solid and Vlasov) are shown in Figures 13 through 16, for one of the cases analyzed. These figures indicate that the Vlasov model is an improvement over the Winkler model, in reproducing the elastic half-space response. The Vlasov option is also substantially less demanding in terms of computer resources than the Elastic Solid.

To determine whether the relation between (E_s, μ_s) and (k, G) is influenced by the thickness of the slab, comparisons between the Elastic Solid and Vlasov models were repeated for a 178 mm (7-in.) slab (compared to the 381 mm (15-in.) slab used in the original "matching" procedure). There was a general deterioration in the agreement between the two models, confirming the observation by Jones and Xenophontos (22) that the flexural rigidity of the plate (and, therefore, its thickness) affect the value of the Vlasov parameters. This realization substantially reduces the feasibility of reproducing elastic solid results by the Vlasov model on a routine basis.

The effect of a second factor, namely that of slab length, was also investigated. It is already suggested from the thickness effect discussed in the preceeding paragraph, that the relation between the two pairs of parameters will also be influenced to some extent by slab length. For a given slab, altering its thickness, h, automatically changes its radius of relative stiffness, ℓ and, therefore, the value of the ratio (L/ℓ), used to characterize the slab length effect. This was confirmed by results obtained when the slab length is reduced from 457 cm (180-in.) to 329 cm (126-in.). Significant deterioration in the closeness of the "match" between the two models was observed.

Finally, the effect of mesh fineness was considered. Results suggested that mesh fineness has practically no effect on the closeness of the "match" between the two models, indicating that both models are affected equally by this factor.

Figure 9. Effect of mesh fineness on maximum interior bending stress (ILLI-SLAB two-parameter option).

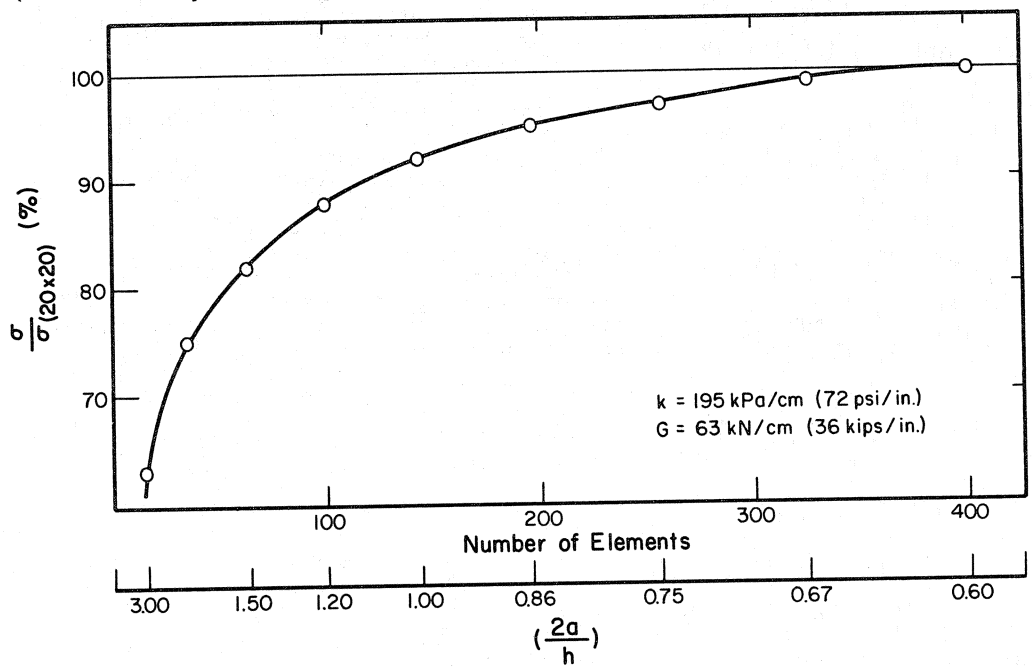

Figure 10. Effect of k on maximum interior deflection and bending stress (ILLI-SLAB two-parameter option).

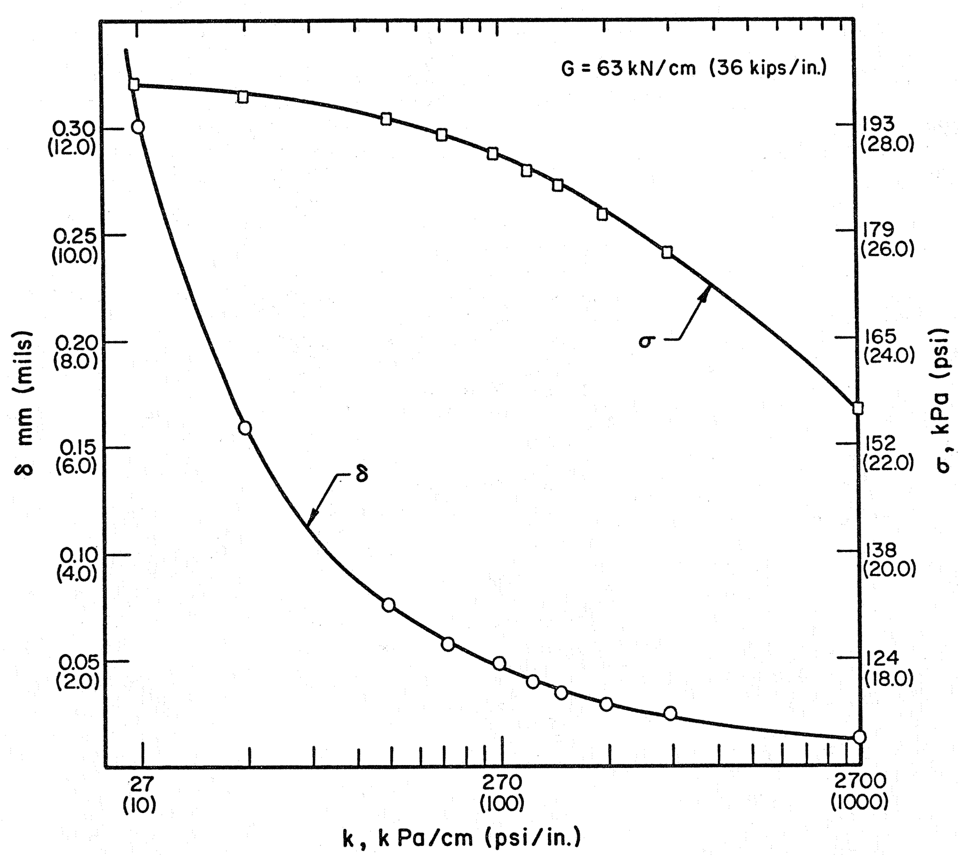

Figure 11. Effect of k on interior loading deflection and bending stress profiles (ILLI-SLAB two-parameter option).

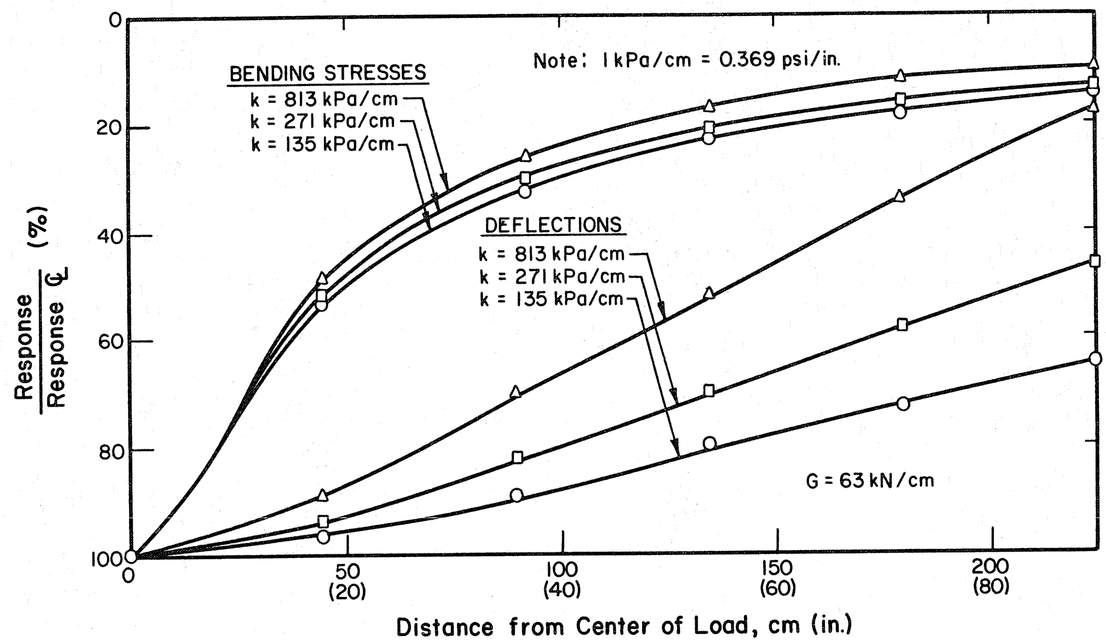

Figure 12. Effect of G on interior loading deflection and bending stress profiles (ILLI-SLAB two-parameter option).

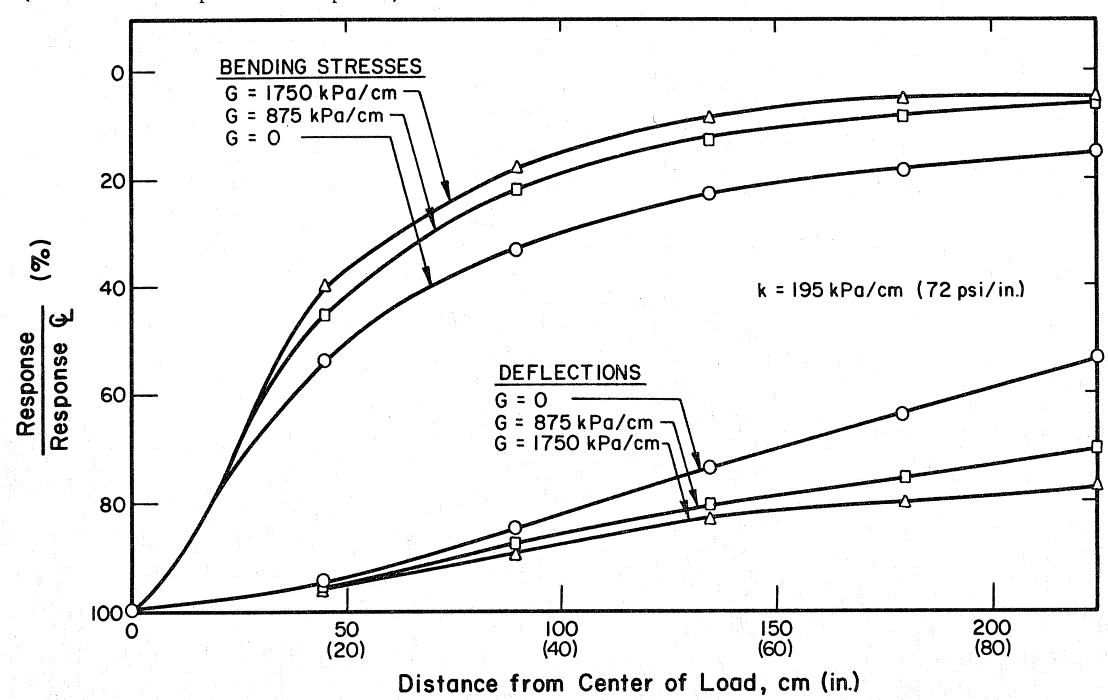

Figure 13. Comparison of deflection profiles (interior loading).

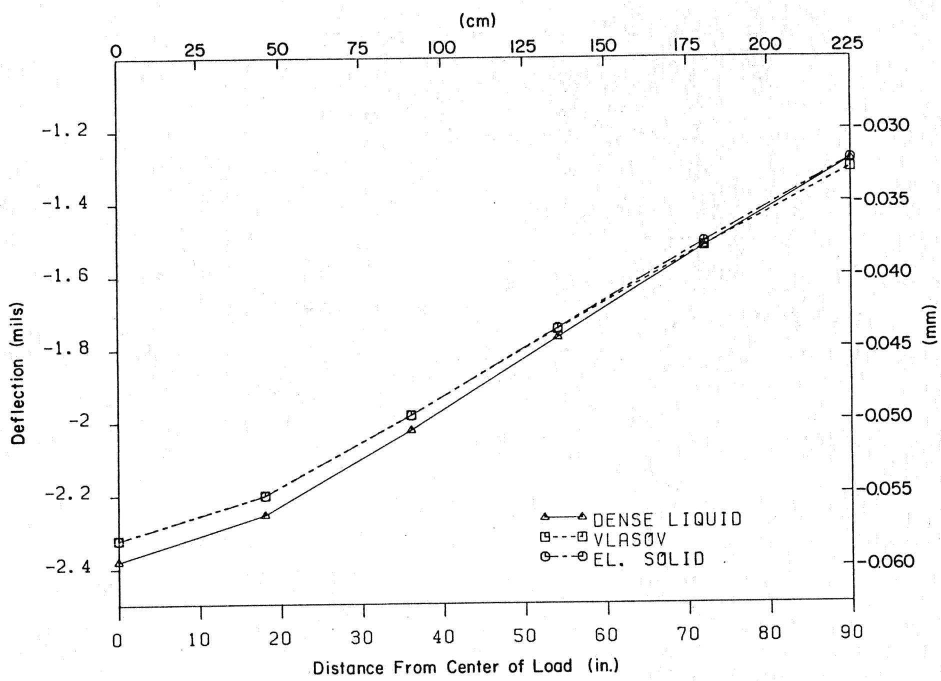

Figure 14. Comparison of subgrade stress profiles (interior loading).

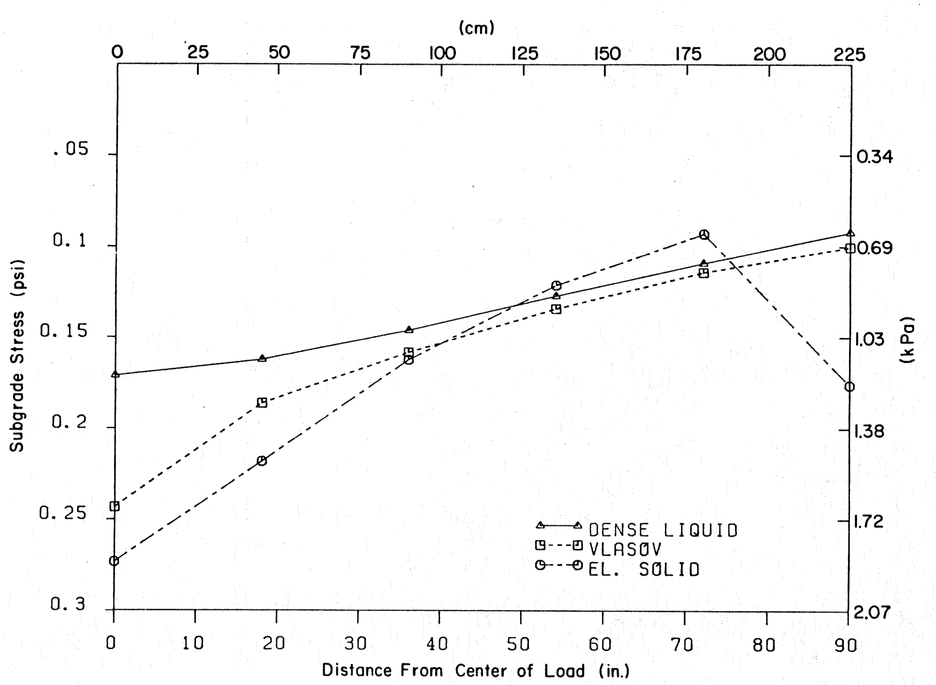

Figure 15. Comparison of bending stress (σ_x) profiles (interior loading).

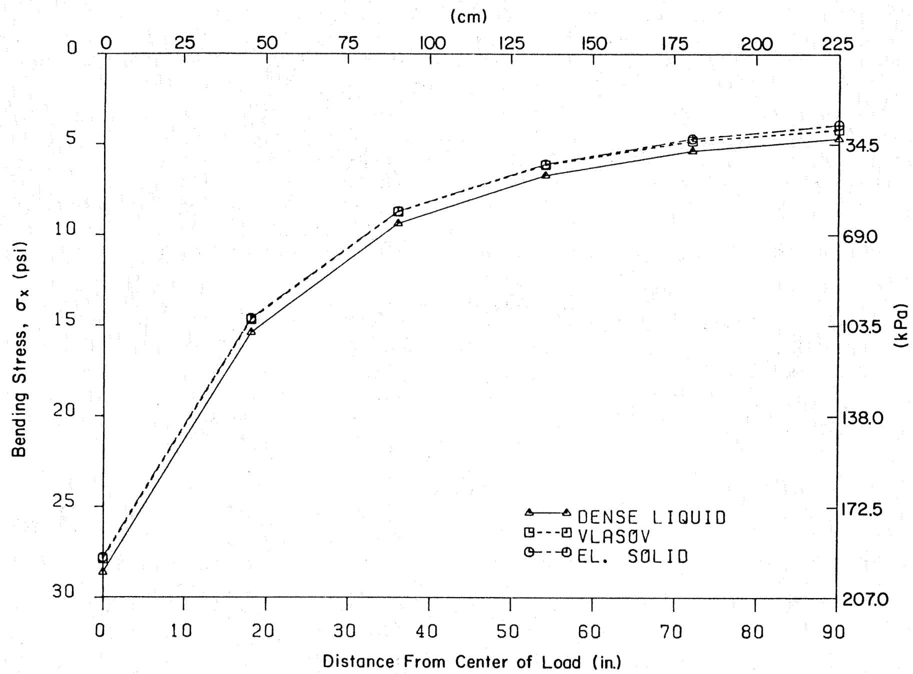

Figure 16. Comparison of bending stress (σ_y) profiles (interior loading).

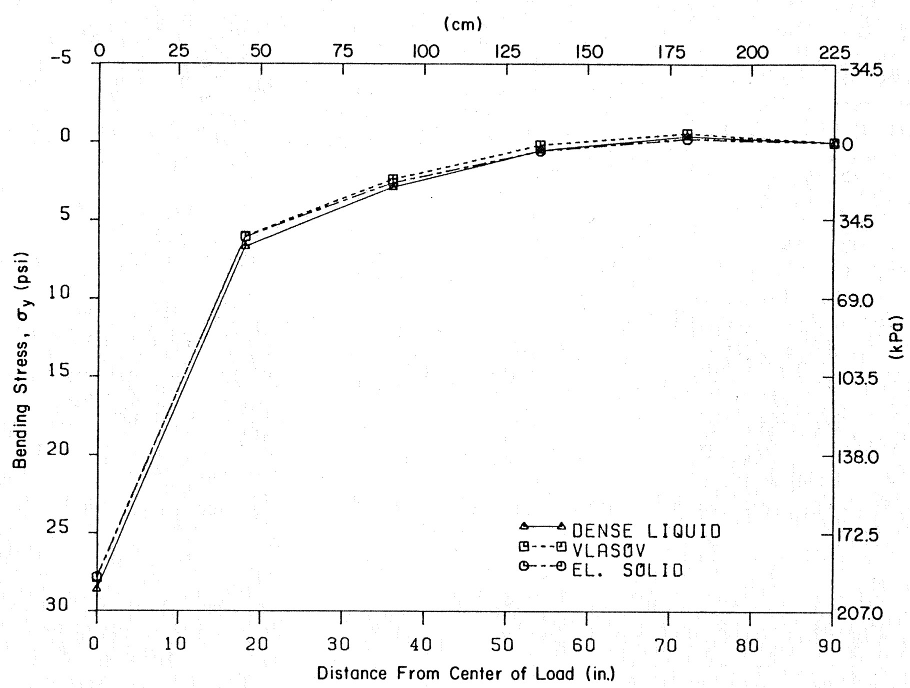

CONCLUSION

A new, revised and expanded version of ILLI-SLAB has been developed. ILLI-SLAB is a finite element program code for the analysis of slab-on-grade pavements. In addition to the original dense liquid formulation, three new models have now been incorporated into ILLI-SLAB to provide the capability to analyze a slab on a stress dependent (resilient) subgrade, a semi-infinite elastic solid, and a two-parameter (Vlasov) foundation. Comparative studies are greatly facilitated, and the whole spectrum of possible subgrade idealizations can be examined, from the entirely discontinuous dense liquid, to the totally continuous elastic solid. The efficient and fruitful utilization of ILLI-SLAB is ensured by adherence to guidelines established during several convergence studies presented in this paper.

Acknowledgments

The investigations for this Paper were conducted under a Research Project sponsored (Grant No. AFOSR-82-0143) by the Air Force Office of Scientific Research (AFOSR), Air Force Systems Command, Bolling AFB, DC. Lt. Col. L.D. Hokanson was the Program Manager.

References

1. A. M. Tabatabaie and E. J. Barenberg. Structural Analysis of Concrete Pavement Systems. Transportation Engineering Journal, ASCE, Vol. 106, No. TE5, September, 1980.
2. O. C. Zienkiewicz. The Finite Element Method. 3rd Edition, McGraw-Hill, 1977.
3. D. J. Dawe. A Finite Element Approach to Plate Vibration Problems. Journal of Mechanical Engineering Science, Vol. 7, No. 1, 1965.
4. A. M. Tabatabaie, E. J. Barenberg, and R. E. Smith. Longitudinal Joint Systems in Slip-Formed Rigid Pavements, Volume II -- Analysis of Load Transfer Systems for Concrete Pavements. U.S. Department of Transportation, Report No. FAA-RD-79-4, II, November, 1979.
5. M. R. Thompson, A. M. Ioannides, E. J. Barenberg and J. A. Fischer. Development of a Stress Dependent Finite Element Slab Model. U.S. Air Force Office of Scientific Research, Report No. TR-83-1061, Air Force Systems Command, USAF, Bolling AFB, D.C. 20332, May, 1983.
6. A. M. Ioannides. Analysis of Slabs-On-Grade for a Variety of Loading and Support Conditions. Ph.D. Thesis, University of Illinois, Urbana, 1984.
7. A. M. Ioannides, E. J. Barenberg, and M. R. Thompson. Finite Element Model with Stress Dependent Support. TRB, Transportation Research Record 954, 1984.
8. J. A. Fischer, M. R. Thompson, A. M. Ioannides, and E. J. Barenberg. K_R - The Resilient Modulus of Subgrade Reaction. TRB, Transportation Research Record 954, 1984.
9. L. Raad and J. L. Figueroa. Load Response of Transportation Support Systems. Transportation Engineering Journal, ASCE, Vol. 106, No. TE1, January, 1980.
10. M. R. Thompson and Q. L. Robnett. Resilient Properties of Subgrade Soils. Transportation Engineering Journal,ASCE, Vol. 105, No. TE1, January, 1979.
11. Y. K. Cheung and O. C. Zienkiewicz. Plates and Tanks on Elastic Foundations: An Application of Finite Element Method. International Journal of Solids and Structures, Vol. 1, 1965.
12. G. Pickett, et al. Deflections, Moments and Reactive Pressures for Concrete Pavements. Bulletin No. 65, Engineering Experiment Station, Kansas State College, October, 1951.
13. J. R. Giroud. Settlement of a Linearly Loaded Rectangular Area. Journal of the Soil Mechanics and Foundations Division, ASCE, Vol. 94, No. SM4, July, 1968.
14. A. Losberg. Structurally Reinforced Concrete Pavements. Doktorsavhandlingar Vid Chalmers Tekniska Hogskola, Gotesborg, Sweden, 1960.
15. P. F. Carlton and R. M. Behrmann. A Model Study of Rigid Pavement Behavior Under Corner and Edge Loadings. Proceedings, 35th Annual Meeting, Highway Research Board, Washington, D.C., 1956.
16. V. Z. Vlasov and N. N. Leont'ev. Beams, Plates and Shells on Elastic Foundations. Translated from the Russian (date of original: 1960), NASA-NSF, NASA TT F-357, TT 65-50135, Israel Program for Scientific Translations, 1966.
17. R. T. Severn. The Solution of Foundation Mat Problems by Finite Element Methods. The Structural Engineer, Vol. 44, No. 6, London, June, 1966.
18. A. D. Kerr. On the Derivation of Well Posed Boundary Value Problems in Structural Mechanics. International Journal of Solids and Structures, Vol. 12, 1976.
19. T. Y. Yang. A Finite Element Analysis of Plates on a Two Parameter Foundation Model. Computers and Structures, Vol. 2, No. 4, 1972.
20. J. Donnelly and J. Conroyd. Development of Vlasov Subgrade Finite Element Model. University of Illinois, 1984 (unpublished).
21. M. A. Mahanyi. Plates on Elastic Layers. Ph.D. Thesis, University of Illinois, Urbana, 1962.
22. R. Jones and J. Xenophontos. The Vlasov Foundation Model. International Journal of Mechanical Science, Vol. 19, No. 6, 1977.